Ecological Informatics 66 (2021) 101442

Contents lists available at ScienceDirect

Ecological Informatics

journal homepage: www.elsevier.com/locate/ecolinf

Quantifying the mitigation of temperature extremes by forests and wetlands in a temperate landscape

Charlotte Gohr [a,b,*], Jeanette S. Blumröder [a,b], Douglas Sheil [c,d], Pierre L. Ibisch [a,b]

[a] Centre for Econics and Ecosystem Management, Eberswalde University for Sustainable Development, Eberswalde, Germany
[b] Biosphere Reserves Institute, Eberswalde University for Sustainable Development, Eberswalde, Germany
[c] Forest Ecology and Forest Management Group, Wageningen University & Research, Wageningen, Netherlands
[d] Center for International Forestry Research, P.O. Box 0113 BOCBD, Bogor, Indonesia

ARTICLE INFO

Keywords:
Surface cooling
Climate change mitigation
Ecological indicators
Forests
Land surface temperature
NDVI

ABSTRACT

As a result of ongoing climate change and more frequent heat events, the regulating services of land cover in terms of moderating and mitigating local temperatures are increasingly important. While the reduced temperatures found in forests and wetlands are recognized, their wider contribution to regional landscape cooling remains largely uncharacterized and unquantified. Herein, we propose and test a new method that estimates the temperature response and inertia of landscapes in high temperatures, based on land cover share. In order to achieve this goal, we combined the MODIS daytime land surface temperature (henceforth LST) time series and CORINE land cover data. We classified the time series in two ways, i.e. by stepwise temperature range (−10/−5 °C to +35/+40 °C) and by the occurrence of hot days (days with a mean LST ≥ 30 °C). As an explanatory variable, we developed and used a *greenest pixel composite* of the MODIS normalized difference vegetation index (NDVI) time series. In our study area, covering parts of northeastern Germany and western Poland, the fragmented landscape has heterogeneous temperature patterns, including urban heat islands, warm agricultural areas, cool forests and cold wetlands. We found that at high temperature ranges only forests and wetlands remained comparably cool, with LSTs up to 20.8 °C lower than the maximum LST in the study area. The analysis of land cover shares and LSTs revealed the substantial cooling effect of forests and wetlands in line with increasing land cover share in higher temperature ranges, as well as on hot days. The relation between LST and the NDVI indicated vegetation cover as the cause. We propose the corresponding metrics to quantify landscape-level temperature regulation. Equally, we advocate for management to identify these ecosystem services and their current and potential contributions, along with implications for sustaining and increasing, both tree cover and wetlands and thereby adapting landscapes to climate change.

1. Introduction

Increases in temperature, which are among the most dangerous impacts of climate change, threaten socioeconomic activities (Chen et al., 2020), ecosystem functioning (Fisher et al., 2017) and human health (Luber and McGeehin, 2008; Mora et al., 2017). Human mortality estimates based on data from climate-related heat exposure and deaths in 732 locations over 43 countries suggest a mean of 37.0% (range 20.5–76.3%) between 1991 and 2018, with increased mortality seen on all continents (Vicedo-Cabrera et al., 2021). Heat also contributes to other climate-related challenges such as increased water-stress and drought (Fisher et al., 2017; Teuling et al., 2013). One way to avoid these negative effects is to prevent or moderate temperature extremes (Hatfield and Prueger, 2015).

The relationship between remotely sensed *land surface temperature* (LST) and land cover has been investigated in various contexts (Alkama and Cescatti, 2016; Bonan, 2008; Bright et al., 2017; Jin and Dickinson, 2010). Different land covers are associated with different thermal properties, especially the heat island effects that occur in urban and other built-up areas (Bartesaghi-Koc et al., 2020; Feizizadeh and Blaschke, 2013; Liu et al., 2018; Su et al., 2010; Tran et al., 2017). Land cover proportion has been used in a study of an urban area to investigate to what extent landscape metrics can explain LST (Liu et al., 2018), as well as for a vegetation fraction cover analysis (Duveiller et al., 2018;

* Corresponding author at: Schicklerstr. 5, 16225 Eberswalde, Germany.
E-mail address: charlotte.gohr@hnee.de (C. Gohr).

https://doi.org/10.1016/j.ecoinf.2021.101442
Received 5 July 2021; Received in revised form 22 September 2021; Accepted 27 September 2021
Available online 1 October 2021

Schwaab et al., 2020). However, the response of hot-day LSTs in relation to land cover shares at different temperature ranges with a focus on multiuse landscapes with urban, forest and agricultural land rather than urban landscapes has not been studied to date.

Greenness, or vegetation productivity measured via the *Normalized Difference Vegetation Index* (NDVI), is commonly applied to quantify and substantiate the impacts of different land cover types on LST. In this regard, a correlation between LST and the NDVI has been detected in various studies (Weng et al., 2004; Xiao and Weng, 2007; Yuan and Bauer, 2007). Vegetated areas with high NDVI show lower LSTs (Deng et al., 2018). The NDVI provides insights into the condition of the vegetation and serves as an explanatory variable for measured LST (Su et al., 2010).

The use of LST to scrutinize the cooling function of forests is well established, as seen in a global study that compared LST and station air temperatures (Mildrexler et al., 2011). Equally, the moderate cooling of temperate forests in summer was observed in a global study using MODIS LST (Li et al., 2015). LST observations have also confirmed cooling resulting from afforestation in China (Peng et al., 2014), while a study of restored oak woodland in Canada found LST declined as the forest matured (Hamberg et al., 2020). Higher LSTs were found following a decline in forest cover due to bark beetle attack following drought conditions in the Czech Republic, thereby demonstrating the utility of remotely-sensed LSTs: rising temperatures in drought-damaged forests led to advection effects and extracted water vapor from the landscape, further promoting landscape desiccation (Hesslerová et al., 2018). In various case studies in Germany, it has been shown that surface temperatures are a good indicator for assessing the functioning of forests and the influence of land use as well as edge effects (e.g. Blumröder et al., 2019a, 2019b; Blumröder et al., 2020; Blumröder et al., 2021; Ibisch et al., 2019).

The threat of high temperature extremes on plants is evident in the drying effect as a result of high air temperatures that absorb more water, while at the same time plants have an increased vapor pressure deficit and atmospheric water vapor demand (Hatfield and Prueger, 2015; Hesslerová et al., 2018). In forest ecosystems, increasing vapor pressure deficit has been linked to increased tree mortality (Breshears et al., 2013; Grossiord et al., 2020; Williams et al., 2013). At the same time, water evaporation from vegetation is an important source of atmospheric moisture (Sheil, 2018). Total water vapor emissions from forests (combined transpiration and evaporation from other sources) are typically higher than for other vegetation, and they can be even higher than for open water (Sheil, 2018). Maintaining cool and healthy forests is also important for preserving microclimatic refuges for many organisms threatened by climate change (Suggitt et al., 2011), while the cooling effects of vegetation contribute to ecosystem-based adaptation and nature-based solutions to heat stress (Bright et al., 2017).

Wetlands, in this study referring equally to water bodies and marshes, influence regional temperatures and play a major role as an ecosystem service in regulating regional climates (Hesslerová et al., 2019; Ramsar Convention Secretariat, 2018; Pokorný et al., 2016). The general cooling function of wetlands in high temperatures is caused by its albedo and evaporation characteristics (Hesslerová et al., 2019). These biophysical processes are not only relevant regarding climate change but functioning wetlands also have a positive effect on the carbon circle and greenhouse gas emissions (Pokorný et al., 2016).

The loss of wetland cover globally is increasing, primarily as a result of human activities (Ramsar Convention Secretariat, 2018). Using remote sensing data, regional studies in China have determined that marshland loss implies warmer local LST (Shen et al., 2020) whereas maintained water bodies and their surroundings have lower LSTs than adjacent urban areas and thereby decrease the UHI effect (Wu and Zhang, 2019). On a global scale, an LST-based analysis distinguished between the regional cooling effect of wetlands in tropical regions throughout the year and seasonal effects in boreal regions with warming effects in winter and cooling effects in summer (Wu et al., 2021). More generally, it is important to understand and foster the daytime cooling capacity of different land covers, particularly when the key factors can be modified through management.

In this paper, we examine the landscape-scale influence of forests and wetlands on moderating high temperature events by applying a new method that relates land cover share to temperature range and to hot days. We use spatial time series based on the large-scale remote sensing data of land surface temperature, classified into temperature ranges and a hot-day composite, to investigate temperature changes in relation to increasing forest and wetland cover. We investigate land cover specific greenness (NDVI) as a possible cause of spatial temperature patterns, and we also discuss the integration of this ecosystem service regulating temperature into landscape management planning.

2. Material and methods

2.1. Study area

We chose a landscape in northeastern Germany sitting on the border with Poland (10,726.8 km^2) and about 100 km south of the Baltic Sea. There is a pronounced land use gradient from the metropolitan region of Berlin in the south to rural ecosystems in the north, comprising both intensively managed agricultural areas and forested regions (Fig. 1). For a European lowland area, the region is quite unique, as within a range of 100 km there is both a large urban area and a forest-dominated landscape, including smaller patches of old-growth forests. In the cultural landscape of the northeastern part of the state of Brandenburg and southeastern Mecklenburg Western Pomerania, large agricultural areas and forests dominate. Roughly 70% of the forest area is dominated by Scots pine (*Pinus sylvestris* L.) plantations, and only smaller parts of the native deciduous broad-leaved forest comprise old-growth forest, most of which is dominated by beech (*Fagus sylvatica* L.) (Ibisch et al., 2018). There are a few scattered lakes of postglacial origin. The soil pattern in the study area is relatively homogenous (Panagos, 2006; Van Liedekerke et al., 2006), and the topography is characterized by small differences in altitude in the range of −10 and 168 m above sea level and a mean slope value of less than 1.7% (Jarvis et al., 2008) (Appendix 1).

2.2. Satellite imagery

We used three preprocessed datasets to examine LST, the NDVI and land cover. Surface temperature information was taken from MODIS (Moderate Resolution Imaging Spectroradiometer) satellite data (Table 1). MODIS is a radio spectrometer on board NASA's Aqua EOS-PM1 satellite, which produces images of the Earth's surface over a wide spectral range and thus allows, among other things, a large-scale investigation of the radiation budget. From the measured radiation intensity in the infrared range (bands 31 & 32 with 10.8–12.3 μm), daily surface temperature is calculated at a resolution of about 1 km, taking into account emissivity and the water vapor content of the air column with the help of the "Generalized Split Window Algorithm" (Wan et al., 2015).

Surface temperature results from various factors such as albedo or emissivity, and it can be locally heterogeneous. Land surfaces can heat up much more during the day than the air above (station air temperature), but there is usually a continuous exchange of heat (Jin and Dickinson, 2010; Mildrexler et al., 2011).

NDVI data was also acquired from a MODIS time series (Table 1). The NDVI is calculated by using the near-infrared and visible spectra provided by satellite imagery, with a 1 km resolution ranging from −1 to 1 (Didan, 2015).

Land cover information was derived from the CORINE dataset of the European Environment Agency's Copernicus program (CORINE: Coordination of Information on the Environment; Table 1). Areas coded in the CORINE dataset as "non-irrigated land" and "pastures" are henceforth referred to as "agricultural land", and areas coded as

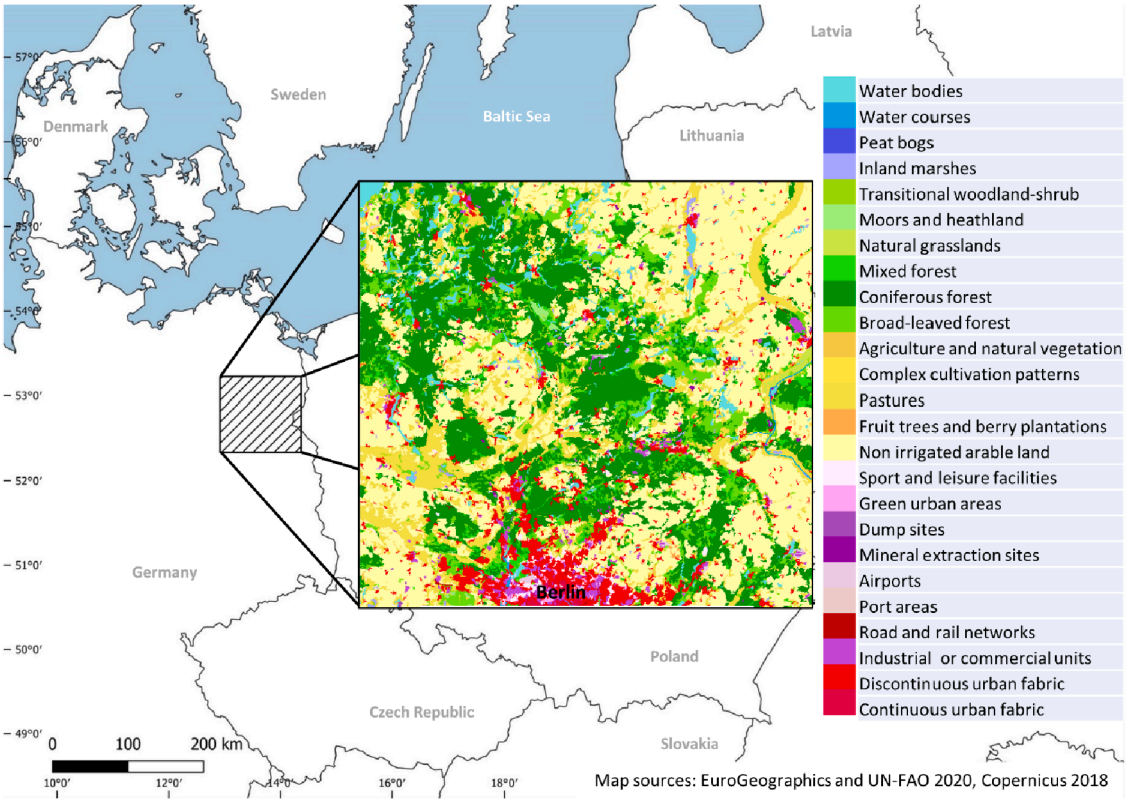

Fig. 1. Map showing the location of the study area (10,726.8 km^2) and its corresponding land cover types.

Table 1
Properties of the used datasets.

Sensor, provider and product ID	Spatial resolution	Temporal coverage	Selected time series	Sequence and time of recording	Number of images
MODIS Aqua, NASA, MYD11A1.006, LST[a]	1 km	04.07.2002 to 13.08.2021[a]	04.07.2002 to 31.12.2020	Time series, 1 day, ~1.30 pm	6618
MODIS Aqua, NASA, MYD13A2.006, NDVI[b]	1 km	04.07.2002 to 20.07.2021[b]	04.07.2002 to 31.12.2020	Time series, 16-day composite, ~1.30 pm	426
Copernicus, EEA, Corine Land Cover[c]	100 m	1990, 2000, 2006, 2012, 2018	2018	Snapshot 2018	1

[a] (Wan et al., 2015). Available time resolution state 17.08.2021. doi:https://doi.org/10.5067/MODIS/MYD11A1.006
[b] To generate the 16-day NDVI composite, the product is run through an algorithm that selects the best pixel with low clouds, a low view angle and the highest NDVI value (Didan, 2015). Available time resolution state 17.08.2021. doi:https://doi.org/10.5067/MODIS/MYD13A2.006
[c] (Copernicus, 2018). https://developers.google.com/earth-engine/datasets/catalog/COPERNICUS_CORINE_V20_100m

"discontinuous urban fabric" and "industrial or commercial units" are henceforth referred to as "urban areas". If not stated otherwise, "forest" is a summary of areas coded as "broad-leaved", "coniferous" and "mixed" forest. The different water body types ("water bodies", "water courses", "inland marshes") are summarized under the term "wetlands".

2.3. Data-processing and statistical analysis

For data acquisition, data-processing and statistical analysis, we used the Google Earth Engine (Google, 2021; Gorelick et al., 2017) as well as the integrated development environment R (R Core Team, 2021).

We generated the temperature range dataset by filtering the mean LST of each image in the whole MODIS LST time series, sorting them stepwise by 5 °C temperature ranges (−10/−5 °C to +35/+40 °C) and calculating a per-pixel mean image for each temperature range. This resulted in ten images with mean values associated with the ten temperature ranges.

The analysis of extreme weather conditions focuses on "hot days" occurring in the period July 2002 – December 2020. The definition of a "hot day" follows Germany's national meteorological service (Deutscher Wetterdienst, DWD), i.e. a maximum air temperature of at least 30 °C (DWD, 2021). In our study, a "hot day" is an image with at least one LST pixel value ≥30 °C. Although the number of days with LST data ≥30 °C is most likely higher than the number of days with corresponding air temperatures, LST data with the chosen threshold represent extreme temperatures at the surface and are therefore suitable for our approach. We reduced the resulting MODIS LST time series with only hot days to a single image with the per-pixel mean of all hot days, which we henceforth refer to as the *hot day composite*.

To quantify the cooling capacities of different land cover types on hot days, we examined the hot-day LST range per land cover type across the area. Land cover changes between 2000 and 2018 were negligible (Appendix 2), so we combined the *hot day composite* (2002−2020) with the land cover data from 2018. The study area includes 13,300 LST pixels at a 1 km resolution, with each pixel comprising approximately 155 land cover pixels at a 100 m resolution. To identify possible differences between land cover types, we grouped and plotted hot-day LSTs per land cover type, attributing LSTs to all land cover shares ranging

from 0 to 100%. We also modelled scenarios in which 1, 5 and 10% of agricultural land is replaced by forest to determine whether the temperature in the study area is affected (Appendix 3). For this purpose, the influence on the mean hot-day LST in the study area was calculated when pixels with 100% agricultural land share were replaced by 100% forest. To quantify the cooling capacities of forests and wetlands, we selected temperature pixels consisting of forests and wetlands with a cover share of ≥50%, thereby illustrating the varying ranges of hot-day LSTs for increasing land cover share from 50 to 100%, without the substantial impacts of mixed pixels with shares between 0 and 50%. For simplicity, we focus on single land covers and omit LST responses due to mixed land cover shares.

To search for LST patterns and land cover share across all temperature ranges, we generated 10 mean images per temperature range (−10/−5 °C to +35/+40 °C) and combined them with the land cover image. For each temperature range, we chose all LST values with a forest or wetland cover share of ≥50% and generated linear models for each land cover type and its associated temperature range. This allowed us to compare the linear model coefficients (the slope representing the relation between LST and land cover share increase) of each land cover type per temperature range.

We used the NDVI to examine possible explanations for dissimilarities in hot-day LSTs for different land cover types. However, the NDVI time series is not processed using the hot-days approach, since a distorted picture of vegetation may arise during heat stress. Therefore, we averaged the "greenest" pixels (i.e. the highest NDVI value) of the 16-day summer month composites (June, July, August) in the MODIS NDVI time series 2002–2020 for our region (henceforth the *greenest composite*).

We combined the *hot day composite* (averaged LST image of hot days), the *greenest composite* and the land cover image to find temperature regulation patterns in the study area. We selected only LST and NDVI values with land cover shares ≥50%. For comparison, we centered (subtracted the mean per value) and scaled (divided the standard deviation per value) LST and the NDVI. To determine if LST varies significantly between different land cover types, we performed an analysis of variance (ANOVA). To clarify possible covariance between land cover and the NDVI in explaining LST, we additionally performed an analysis of co-variance (ANCOVA). For a spatial analysis of LST and the NDVI in forested areas, we produced a bivariate map for areas with a ≥ 50% forest share, using the averaged LST image for hot days and the greenest NDVI image.

3. Results

3.1. Landscape temperatures

Deviation in the mean LST indicated land cover-related patterns across the study area for each temperature range considered herein (Fig. 2). Berlin - in the south - was consistently warmer across all temperature ranges. In the higher temperature ranges, from 10 to 15 °C upwards, forests and wetlands tended to show below-average variations, indicating that the heating of these systems lags behind other parts of the landscape. This delayed response allows temperature differences between the faster heating (warmest) and slower heating (coolest) pixels to increase in the higher temperature bands. In the hottest temperature range (35–40 °C), the LST difference between the hottest pixel (44.1 °C) and the coolest pixel (23.3 °C) reached 20.8 °C.

3.2. Land cover shares and temperature effects

The regional distribution of hot-day LST values in relation to the percentage of forest and wetland coverage per pixel indicated a significant negative relationship (Fig. 3). The strongest signal can be observed for wetlands (slope −7.98), followed by coniferous and broad-leaved forests. Data for mixed forests is relatively sparse and yielded no clear pattern (slope 0.36).

Similar patterns were observed when relating the land cover share gradient (= temperature change with increasing share of one land cover from 50 to 100%) to temperatures summarized in 5 °C stepwise temperature ranges, from −10/−5 °C to +35/+40 °C (Fig. 4). The linear model coefficient (LST ~ land cover share) was depicted for differentiated and summarized land cover types per temperature range. With increasing temperatures, the lm-coefficient became increasingly negative for wetlands, as well as, albeit to a lesser extent, for broad-leaved and coniferous forests (Fig. 4 A). The summarized land cover types indicated negative slopes for forests and wetlands when temperatures rise, whereas agricultural and urban areas showed a positive slope with rising temperature ranges (Fig. 4 B).

The *hot day composite* (mean image of the selection of hot-day LSTs

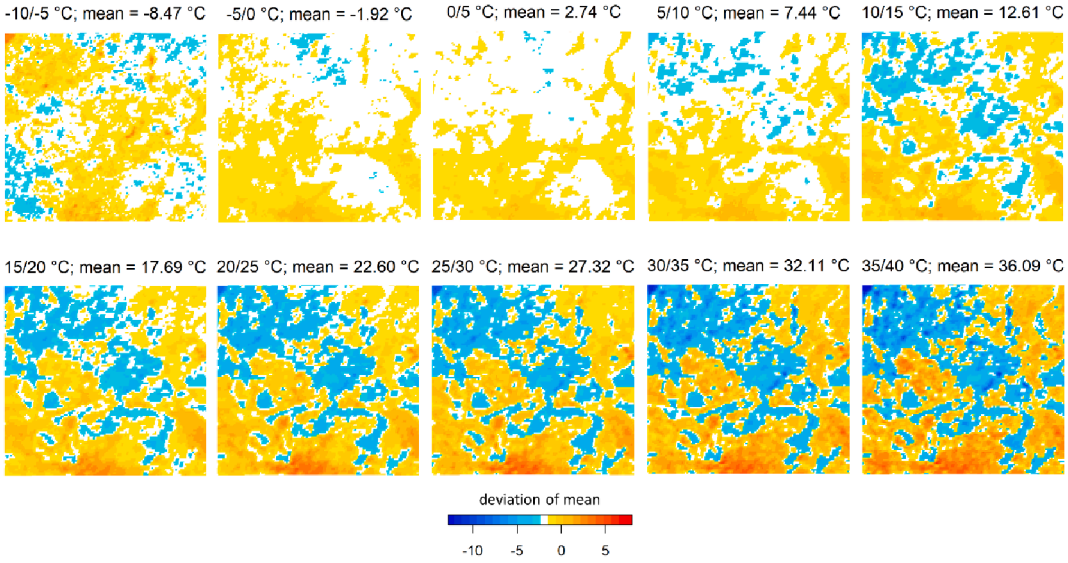

Fig. 2. Ten temperature ranges between −10 and − 5 °C and 35 and 40 °C in 2002–2020 for the study area (as per Fig. 1), showing the per-pixel deviation of mean LSTs. The respective mean value of each range is depicted in white, negative deviations (LSTs cooler than the mean) are blue and positive deviations (LSTs warmer than the mean) are red. For scale and locations, see Fig. 1. (For interpretation of the references to colour in this figure legend, the reader is referred to the web version of this article.)

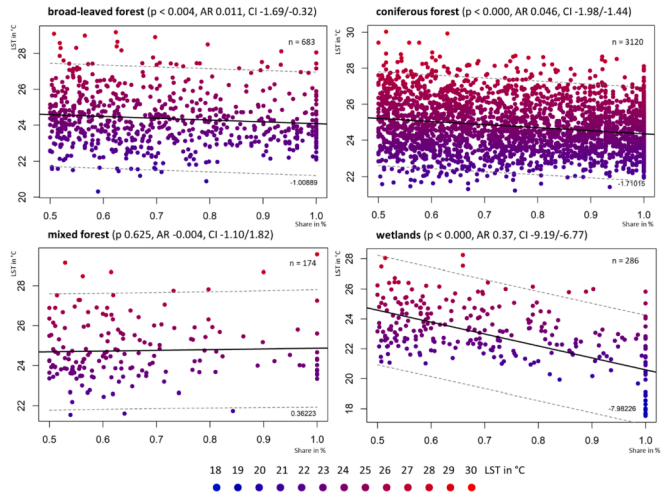

Fig. 3. Hot-day LST values in °C by shares of forest and wetland cover from a 50% to a 100% share. Each LST pixel comprises ~155 land cover pixels. Each LST value is related to the share of each land cover type per LST pixel. 'p' is the probability, 'AR' is the adjusted R-squared and 'CI' is the 95% confidence interval. Numbers of observations ('n') and the slope of the linear model are depicted in the plot.

with at least one regional value ≥30 °C) revealed an anticipated pattern with higher LSTs in urban areas and lower LSTs in forests and wetlands, using all land cover shares ranging from 0 to 100% (Fig. 5 A). Urban areas, i.e. industrial areas, settlements and non-contiguous urban areas, as well as agricultural areas showed values well above 26 °C, while forests (deciduous, coniferous and mixed) and wetlands were between 22 and 25 °C.

The study area comprises 6.6% continuous forest and 13.9% continuous agricultural land. When modelling the replacement of 1%, 5% and 10% forest with agricultural land, a change in the mean temperature on hot days is evident in the study area (Fig. 5 B, Appendix 3). A 10% increase in forest cover would lead to an estimated decrease of 0.9 °C in the mean temperature on hot days in the study area.

3.3. LST and the NDVI

Scaled values for the *hot day composite* and the greenest NDVI image were inversely related (Fig. 6). Only LST and NDVI values with ≥50% of one land cover type were included in the analysis. Urban areas indicated high LST and low NDVI values, whereas forests and wetlands indicated a reverse dispersion with a high NDVI and low LST. Weaker variances in LST and NDVI values were captured for agricultural land, while differences between LSTs for land cover types were significant (ANOVA, $n = 13{,}300$, $p < 0.000$). ANCOVA testing (Type III for unbalanced designs) revealed that with and without land cover as a co-variable, the NDVI had a significant relationship with LST (n = 13,300, $p < 0.000$).

Bivariate mapping of the distribution of LST and the NDVI for pixels with a ≥ 50% share of all forest types revealed a distinctive pattern (Fig. 7). Forest areas in the northwest of the area were cold and high in

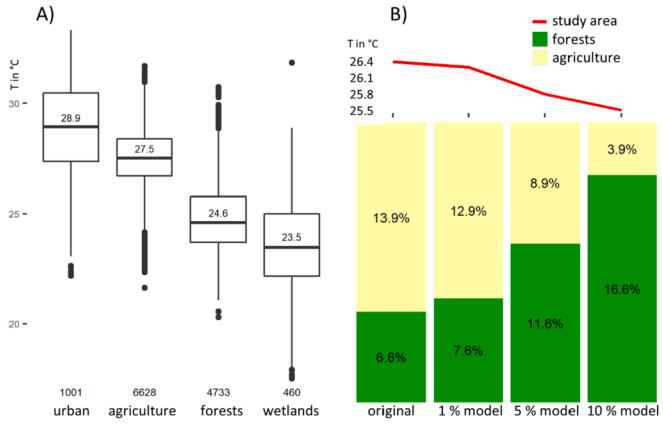

Fig. 5. A) Temperatures comprising different land cover types on days with a maximum temperature ≥ 30 °C (*hot day composite*) in the study area. Pixel count per class is indicated on the x-axis. Median value per class is depicted in each boxplot. B) Coverage and temperature changes in the study area for three models. Bars show scenarios when forests replace agricultural land by 1, 5 and 10%. Line plot shows the declining *hot day composite* temperature in the study area up to 0.9 °C with respective forest cover gain.

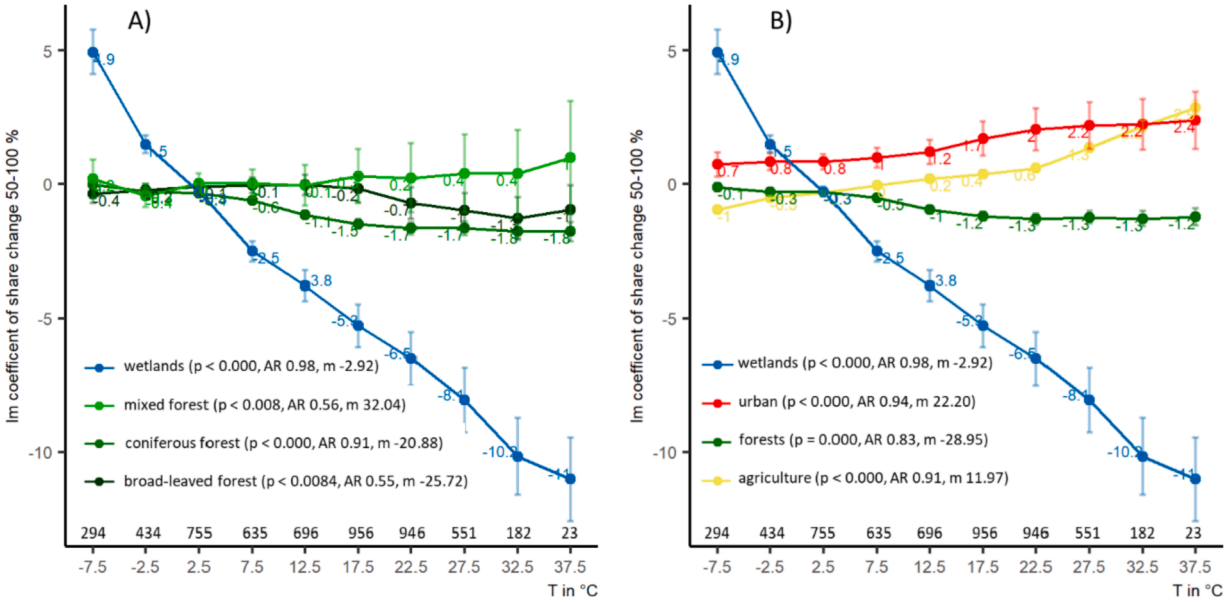

Fig. 4. Relation between the linear model coefficient (LST/range ~ 50–100% share) in stepwise ranges of 5 °C from −10/−5 °C to 35/40 °C for different land covers. Linear model 95% confidence intervals are depicted for each land cover type coefficient in its associated temperature range. Image count per temperature range is indicated on the x-axis. 'p' indicates the probability, 'AR' the adjusted R-squared and 'm' the slope of the linear model. A) Diagram of differentiated forest types and wetlands. B) Diagram of summarized land cover groups, namely wetlands, urban areas, forests and agricultural areas.

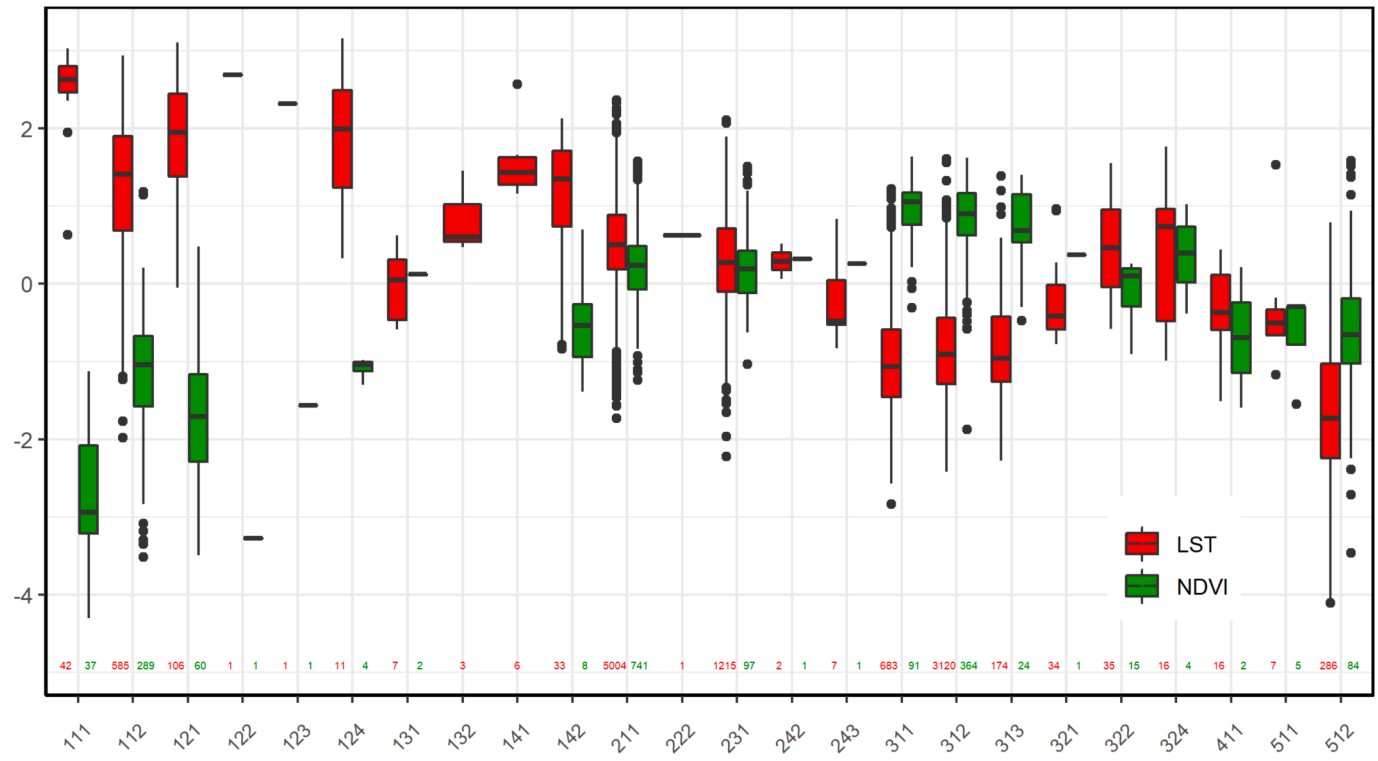

Fig. 6. Scaled distribution of the mean LST of hot days and the greenest NDVI for land cover types with a share of ≥50%. Colored numbers show the numbers of data points per boxplot. Hot-day LSTs are the means of each pixel of the time series 2002–2020 with a daily mean LST ≥ 30 °C. *Greenest composite* NDVI are the maximum values of each pixel of a time series 2002–2020 for the summer months (June, July, August). Both datasets are centered (subtracting the mean per value) and scaled (dividing the standard deviation per value). Designation and order follow the CORINE land cover classification.

greenness (marked in blue), while large conifer plantations at the center of the region were cold but less productive in terms of vegetation (marked in yellow). Smaller forest patches showed a lower NDVI and higher LSTs.

4. Discussion

We have quantified the cooling of landscapes associated with forests and wetlands - or, more precisely, reduced warming - by applying a new method that estimates temperature changes in line with increasing land cover fractions for different temperature ranges. The general temperature mitigation effects of forests and wetlands are consistent with previous studies (e.g. Alkama and Cescatti, 2016; Bonan, 2008; Bright et al., 2017; Frenne et al., 2019; Zellweger et al., 2019). Our quantitative approach is novel, and it demonstrates that we can estimate and manage these contributions and thus moderate temperature extremes across complex landscapes. We now examine the implications of these methods and results.

4.1. Landscape thermal effects of forests and wetlands

We measured daytime thermal effects as the slope of the temperature difference versus the relative share of a specific land cover type per LST pixel for temperatures ranging from −10/−5 °C to +35/+40 °C; all resulting relationships were statistically significant ($p < 0.005$, adjusted R-squared >0.5). Increasing forest cover (all forest types combined, or differentiated by broad-leaved, coniferous and mixed forest) reduces temperatures during heat events compared to other land cover types (Fig. 3 A). Urban areas and agricultural land heat up more (Fig. 3 B), while wetlands reveal the greatest temperature differences at high temperatures and warming at the coldest temperature. Previous studies have established that such thermal reactions in wetlands can be explained not only by albedo and evapotranspiration, but also by soil heat flux, i.e. energy absorbed in the summer and then released in the winter (Shen et al., 2021, 2020; Wu et al., 2021).

We observed that the cooling – or warming – of a given pixel depends on the relative share of each land cover type. The analysis of land cover share influence on hot days (*hot day composite*) indicated that while wetlands have the highest cooling effect when a pixel is 100% covered by wetland (lm coefficient −7.98), coniferous forest (lm coefficient −1.71) and broad-leaved forest (lm coefficient −1.01) also exhibit significantly lower LSTs if the share is closer to 100%. Only the influence of mixed forest (lm coefficient 0.36) was not clearly related to its share (Fig. 3), most likely a result of the lower number of observations leading to inadequate statistical power (Fig. 8). These findings are in congruence with the results of a study that showed how land cover proportion characterizes LST in a Chinese urban landscape (Liu et al., 2018). The stronger influence of coniferous forest in comparison to broad-leaved forest could be a result of more data points and planting densities. However, the absolute values show cooler LSTs in broad-leaved forests than in coniferous forests, which is consistent with a study of forest cover proportions across Europe (Schwaab et al., 2020).

The comparison of *hot day composite* temperatures (landscape mean of a day ≥30 °C) for different land cover types (with 0–100% share) at a scale of 100 m shows that forested areas and wetlands are up to 5 °C cooler than urban areas and agricultural lands (Fig. 5 A). Similar results in the southeastern United States have found that forests are 4–6 °C cooler than grasslands, and air temperatures are 2–3 °C lower (Novick and Katul, 2020). We have not dwelt here on the mechanisms by which this land surface temperature buffering is achieved, but these include both the thermal inertia that results as heat passes from warmer to colder bodies, particularly water, and the energy that is absorbed when water evaporates, both of which rely on the presence of water. The availability of water is of course also influenced by the presence of trees and wetlands and these influences are also potentially complex and involve a range of local to regional scales (Ellison et al., 2017; Sheil,

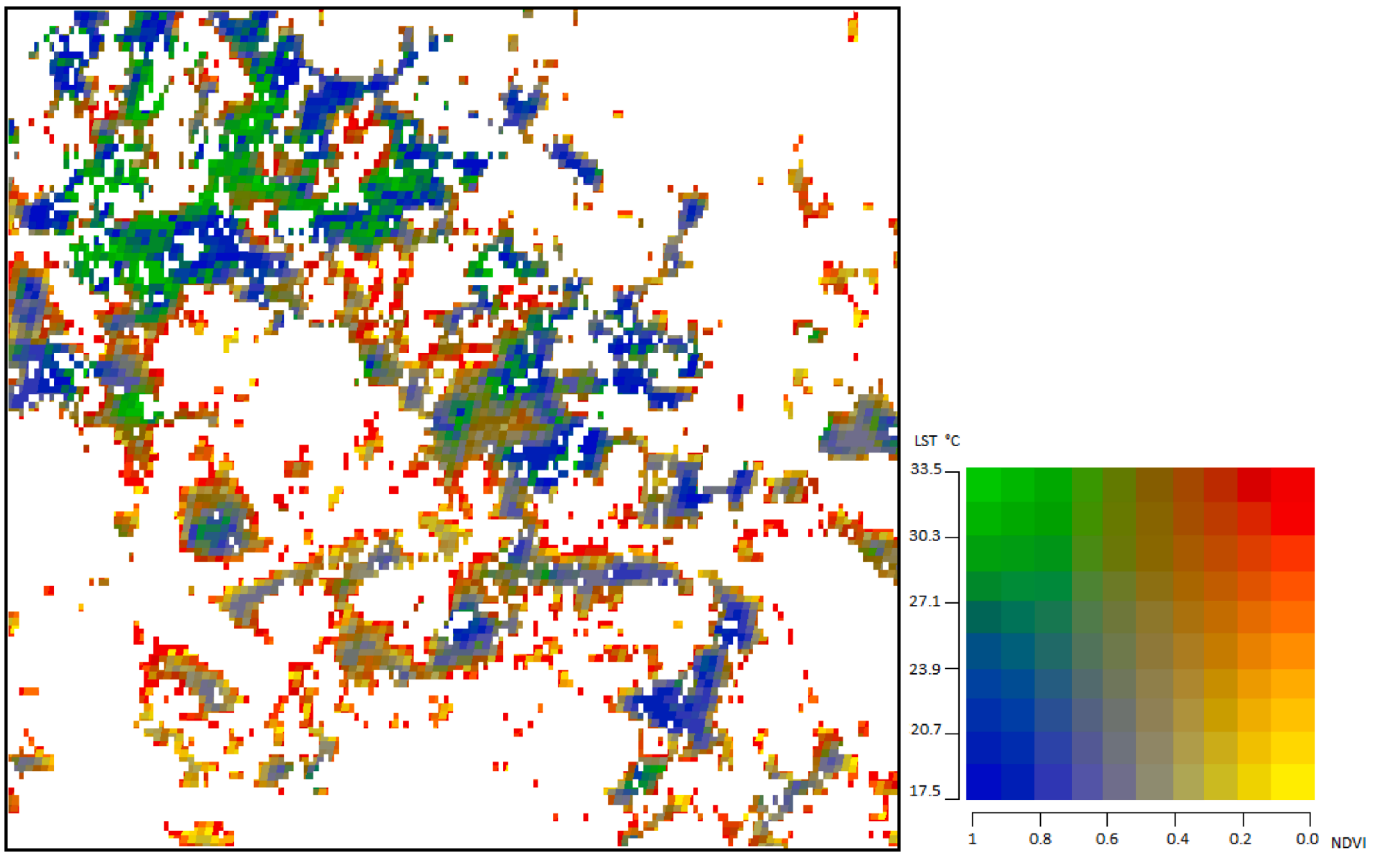

Fig. 7. Bivariate map of LST (means of each pixel of a time series 2002–2020 for hot days) and NDVI (max of each pixel of a time series 2002–2020) of forest areas with ≥50% share. Blue: NDVI high/LST low; Green: NDVI/LST high; Red: NDVI low/LST high; Yellow: NDVI low/ LST low. For scale and locations, see Fig. 1. (For interpretation of the references to colour in this figure legend, the reader is referred to the web version of this article.)

2018). The cooling functions of forests and wetlands at high temperatures are closely linked to ecohydrological functions that support the extraction, recycling and storage of water in the ecosystem (Ellison et al., 2017). Evaporation, transpiration and shade (in forests) offered by forests and wetlands ensure local cooling during the daytime (Ellison et al., 2017; Maes et al., 2011; Shen et al., 2020). However, decreased soil moisture due to heat extremes can interfere with temperature-moderating functions (Teuling et al., 2010). In sum, land cover temperature mitigation provided by forests and wetlands comprises different local and regional factors, such as evaporation, albedo and energy dissipation, as well as supra-regional factors such as landscape land cover composition and clouds (Wu et al., 2021; Shen et al., 2020; Bright et al., 2017; Zeng et al., 2017; Bonan, 2008; Benayas et al., 2008; Zaitchik et al., 2006; Schneider and Kay, 1994).

4.2. Forest cooling, greenness and landscape modelling

The pattern of the *hot day composite* of LSTs and the greenest composite of the NDVI shows contradictory relations for urban areas (high LST, low NDVI) and forests (high NDVI, low LST) (Fig. 6). The ANCOVA test for an effect of the NDVI on LST accounting for land cover types, provides a significant result. As the NDVI and LST are negatively correlated, we conclude that more productive vegetation is associated with a lower LST, and the greenest pixel in a time series provides an indicator for LSTs. The local cooling function of forests is known to be maximized in dense biomass-rich stands (De Frenne et al., 2019; Norris et al., 2012; Zellweger et al., 2019; Schwaab et al., 2020), which is consistent with the results of another study on the island of Madeira, where thermal infrared radiation as a function of LST was used to identify different land cover types. The research determined that older ecosystems with more complex structures have lower average temperatures (Avelar et al., 2020).

Our models suggest that replacing 10% of agricultural land with forest would reduce the mean temperature of the *hot day composite* in the study area by 0.9 °C (Fig. 5 B). It is noteworthy that the models remain conservative estimates, as we neglected edge effects where cooling spills from one pixel to its neighbors - an influence that should be evaluated in future work. In general, an increase in forest area can be achieved by the natural succession of abandoned agricultural land, by planting trees or a combination of both. Benayas et al. (2008) proposed “woodland islets”, i.e. many small afforested areas providing ecosystem services and enhancing biodiversity (Benayas et al., 2008). Investigations into the ability of these “woodland islets” to cool the landscape are necessary in a landscape management seeking cooling functions.

4.3. Implications for ecosystem-based adaptation for climate change

The advancing climate crisis, with the increasing risk of extreme heat events, highlights the importance of maintaining landscapes where extreme temperatures are avoided as much as possible. To study the regulating ecosystem services of forests and wetlands further, we recommend the analysis of hot-day LSTs (days with a mean ≥30 °C in our region) in combination with the greenest pixel NDVI composite. The use of preprocessed spatial data (MODIS LST and NDVI, CORINE land cover) facilitates analysis. However, inaccuracies in spatiotemporal data, such as database errors, topographic characteristics and land cover changes, influence the results and need to be addressed. The spatial resolution of the MODIS Aqua satellite (1 km) is a limitation; however, it is sufficient to detect temperature buffers in our study region. A higher spatial resolution, available from Landsat, ASTER and Sentinel, would

permit assessments on finer scales (e.g. Avelar et al., 2020; Hesslerová et al., 2018; Liu et al., 2018). It is important to note that the measured LSTs are not necessarily the daily maximum values, as the MODIS Aqua satellites take these measurements at around 1.30 pm each day, and the temperature often increases later in the day. This is particularly relevant, because the temperature mitigation of forests and wetlands is even greater in higher temperature bands (Fig. 2). While extreme heat exerts huge stress on ecosystems and people, we see that the presence of forests and wetlands can reduce such impacts (Fig. 3).

The thermal effects of forests and wetlands offer ecosystem-based adaptation, in order to reduce heat stress related to climate change (e.g. Kupika et al., 2019; Nanfuka et al., 2020; Schumacher et al., 2018). Furthermore, forest and wetland loss are therefore not only potential drivers of increasing heat stress, but they also most likely influence relevant biogeochemical functions such as carbon storage and the regulation of greenhouse gas emissions (Laurance et al., 1998; Liu et al., 2019; Pugh et al., 2020; Shen et al., 2020). We need to recognize these functions in landscape management and consider a number of goals and incentives (Lusiana et al., 2017). In addition, further work is required to assess the costs and benefits of different arrangements within a landscape (e.g. Parks and Hardie, 2018). More forests and more wetlands will provide greater adaptation benefits by mitigating extreme heat than any other type of land cover.

5. Conclusion

We quantified the thermal influence of forests and wetlands over a large area north of Berlin, Germany, by developing a novel pixel-based approach. The ability of forests and wetlands to moderate temperatures increases in line with spatial coverage and increased heat. Our approach, using readily available data, accounts for yearly and seasonal variance and shows patterns of expected temperature ranges for all land cover types. Our results highlight the value of forests and wetlands in reducing peak temperatures and thus mitigating some of the more severe impacts of climate change that are increasingly dangerous for human health. Our quantification of landscape cooling is valuable for the analysis of temperate landscapes, and its application could be implemented in other regions, without considerable effort. We recommend that the regulation of ecosystem services, including the avoidance of extreme heat, should play a greater role in landscape planning and management.

Author contributions

PLI, CG and JB designed the research, CG performed the analysis and visualization, CG and PLI wrote the original draft, DS provided comprehensive support in the assessment and interpretation of the results, and all authors contributed to the interpretation of the results and the subsequent revisions of the paper.

Declaration of Competing Interest

None.

Acknowledgements

Funding for this study was provided by the 'BERNAU.Pro.Klima' project by the German Federal Ministry of the Environment, Nature Conservation and Nuclear Safety, grant number 03DAS125. The study was partly funded through the "Gläserner Forstbetrieb" project by the German Federal Ministry for Education and Research (BMBF) via the VDI/VDE, grant number 16LC1603C. PLI conceived and supervised the study within the framework of his long-term research program facilitated by the research professorships "Biodiversity and natural resource management under global change" (2009–2015) and as "Ecosystem-based sustainable development" (since 2015) granted by Eberswalde University for Sustainable Development. CG was funded through the Biosphere Reserves Institute and the Innovation and Career Center "ProBio-LaB" by the Ministry of Science, Research and Culture of the federal state of Brandenburg. We thank Steffen Kriewald for performing the initial calculations and providing the first ideas for this analysis. We also wish to thank two anonymous reviewers for their valuable contributions.

Appendix 1

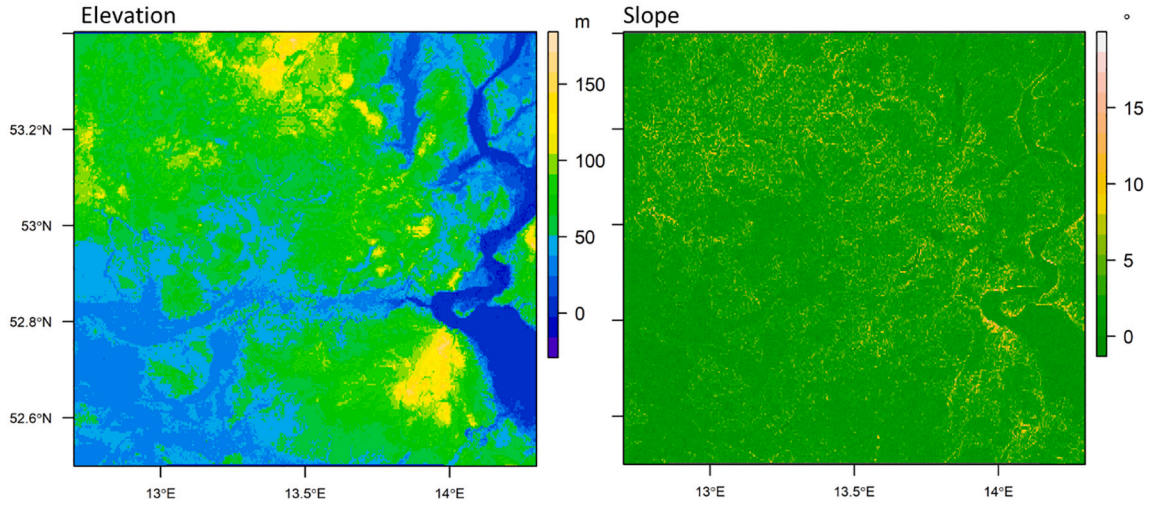

Elevation (range −10 to 168 m) and slope (range 0 to 1.8°) of the study area. More than 70% of areas with a forest cover of >50% lie within an elevation of 50–90 m and with slopes between 0 and 2°.

Appendix 2

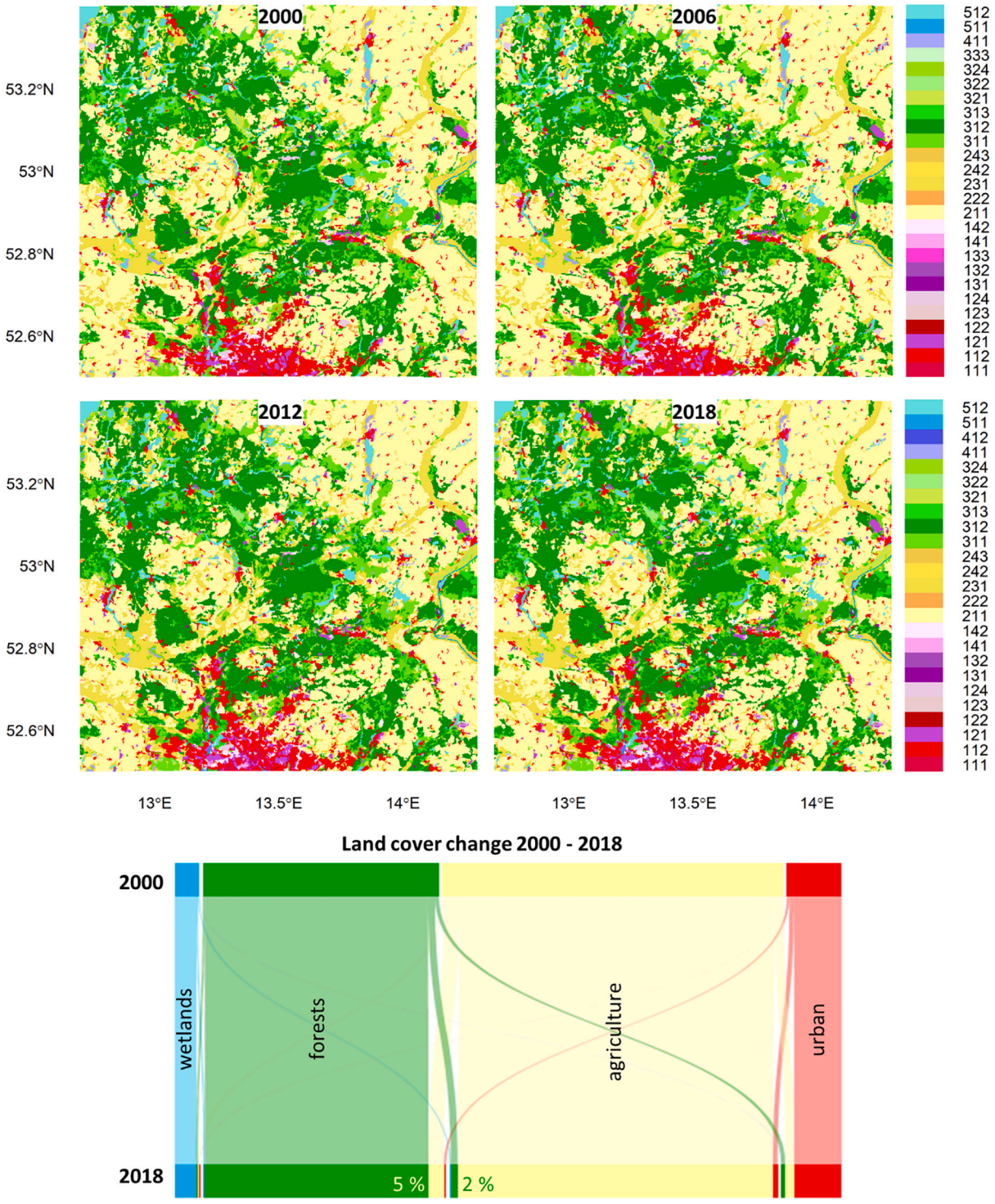

Land cover maps for 2000, 2006, 2012 and 2018. The quantification of land cover change between 2000 and 2018 exhibits no significant changes per land cover type. 2% of forest cover in 2000 was replaced by agricultural land in 2018, whereas 5% of agricultural land in 2000 was replaced by forest cover in 2018. For scale, locations and land cover types, see Fig. 1.

Appendix 3

Coverage and temperature changes for the *hot day composite* in the study area for three models. Respective LST for shares with agricultural land replaced by forest cover by 1, 5 and 10%.

	Study area	Forests 100% share	Agricultural land 100% share	Forests and agricultural land	All land cover types without forest and agricultural land
Share of study area in %	100	6.6	13.9	20.5	79.5
Mean of hot-day LST in °C	**26.4**	24.3	27.8	**26.7**	26.1
1% model: forest for agricultural land	26.3 °C	7.6%	12.9%	26.5 °C	26.1 °C
5% model: forest for agricultural land	26.0 °C	11.6%	8.9%	25.8 °C	26.1 °C
10% model: forest for agricultural land	**25.5 °C**	16.6%	3.9%	**25.0 °C**	26.1 °C

References

Alkama, R., Cescatti, A., 2016. Biophysical climate impacts of recent changes in global forest cover. Science 351 (6273), 600–604. https://doi.org/10.1126/science.aac8083.

Avelar, David, Garrett, Pedro, Ulm, Florian, Hobson, Peter, Penha-Lopes, Gil, 2020. Ecological complexity effects on thermal signature of different Madeira Island ecosystems. Ecol. Complex. 43, 100837.

Bartesaghi-Koc, Carlos, Osmond, Paul, Peters, Alan, 2020. Quantifying the seasonal cooling capacity of 'green infrastructure types' (GITs): an approach to assess and mitigate surface urban Heat Island in Sydney, Australia. Landsc. Urban Plan. 203 (November), 103893. https://doi.org/10.1016/j.landurbplan.2020.103893.

Benayas, José M. Rey, Bullock, James M., Newton, Adrian C., 2008. Creating woodland islets to reconcile ecological restoration, conservation, and agricultural land use. Front. Ecol. Environ. 6 (6), 329–336. https://doi.org/10.1890/070057.

Blumröder, J.S., Burova, Natalya, Winter, Susanne, Goroncy, Agnieszka, Hobson, Peter R., Shegolev, Andrey, Dobrynin, Denis, et al., 2019a. Ecological effects of clearcutting practices in a boreal Forest (Arkhangelsk region, Russian Federation) both with and without FSC certification. Ecol. Indic. 106, 105461. https://doi.org/10.1016/j.ecolind.2019.105461.

Blumröder, J.S., Ibisch, P.L., Kriewald, S., 2019b. Hambacher Forst in Der Krise (II) Temperaturmessungen Zur Beurteilung Der Mikroklimatischen Situation Des Waldes Und Des Randbereichs. Greenpeace e.V, Hamburg.

Blumröder, J.S., Hoffmann, Monika T., Ilina, Olga, Winter, Susanne, Hobson, Peter R., Ibisch, Pierre L., 2020. Clearcuts and related secondary dieback undermine the ecological effectiveness of FSC certification in a boreal Forest. Ecol. Process. 9 (1), 10. https://doi.org/10.1186/s13717-020-0214-4.

Blumröder, Jeanette S., May, Felix, Härdtle, Werner, Ibisch, Pierre L., 2021. Forestry contributed to warming of forest ecosystems in northern Germany during the extreme summers of 2018 and 2019. Ecol. Solutions Evidence 2 (3), e12087. https://doi.org/10.1002/2688-8319.12087.

Bonan, G.B., 2008. Forests and climate change: Forcings, feedbacks, and the climate benefits of forests. Science 320 (5882), 1444–1449. https://doi.org/10.1126/science.1155121.

Breshears, David D., Adams, Henry D., Eamus, Derek, McDowell, Nate, Law, Darin J., Will, Rodney E., Williams, A. Park, Zou, Chris B., 2013. The critical amplifying role of increasing atmospheric moisture demand on tree mortality and associated regional die-off. Front. Plant Sci. 4 https://doi.org/10.3389/fpls.2013.00266.

Bright, Ryan M., Davin, Edouard, O'Halloran, Thomas, Pongratz, Julia, Zhao, Kaiguang, Cescatti, Alessandro, 2017. Local temperature response to land cover and management change driven by non-radiative processes. Nat. Clim. Chang. 7 (4), 296–302. https://doi.org/10.1038/nclimate3250.

Chen, Jie, Liu, Yujie, Pan, Tao, Ciais, Philippe, Ma, Ting, Liu, Yanhua, Yamazaki, Dai, Ge, Quansheng, Peñuelas, Josep, 2020. Global socioeconomic exposure of heat extremes under climate change. J. Clean. Prod. 277, 123275.

Copernicus, 2018. CLC 2018 - Copernicus Land Monitoring Service [Data Set]. https://land.copernicus.eu/pan-european/corine-land-cover/clc-2000.

Deng, Yuanhong, Wang, Shijie, Bai, Xiaoyong, Tian, Yichao, Wu, Luhua, Xiao, Jianyong, Chen, Fei, Qian, Qinghuan, 2018. Relationship among land surface temperature and LUCC, NDVI in typical karst area. Sci. Rep. 8 (1), 1–12.

Didan, K., 2015. MOD13A2 MODIS/Terra vegetation indices 16-day L3 global 1km SIN grid V006 [data set]. NASA EOSDIS Land Processes DAAC. https://doi.org/10.5067/MODIS/MOD13A2.006.

Duveiller, Gregory, Hooker, Josh, Cescatti, Alessandro, 2018. The mark of vegetation change on Earth's surface energy balance. Nat. Commun. 9 (1), 679. https://doi.org/10.1038/s41467-017-02810-8.

DWD, 2021. Wetter Und Klima - Deutscher Wetterdienst - German Climate Atlas. https://www.dwd.de/EN/ourservices/germanclimateatlas/climateatlas_node.html.

Ellison, David, Morris, Cindy E., Locatelli, Bruno, Sheil, Douglas, Cohen, Jane, Murdiyarso, Daniel, Gutierrez, Victoria, et al., 2017. Trees, forests and water: cool insights for a hot world. Glob. Environ. Chang. 43, 51–61. https://doi.org/10.1016/j.gloenvcha.2017.01.002.

Feizizadeh, Bakhtiar, Blaschke, Thomas, 2013. Examining urban Heat Island relations to land use and air pollution: multiple endmember spectral mixture analysis for thermal remote sensing. IEEE J. Selected Topics Appl. Earth Observations Remote Sensing 6 (3), 1749–1756. https://doi.org/10.1109/JSTARS.2013.2263425.

Fisher, Joshua B., Melton, Forrest, Middleton, Elizabeth, Hain, Christopher, Anderson, Martha, Allen, Richard, Matthew F. McCabe, et al., 2017. The future of evapotranspiration: global requirements for ecosystem functioning, carbon and climate feedbacks, agricultural management, and water resources. Water Resour. Res. 53 (4), 2618–2626. https://doi.org/10.1002/2016WR020175.

Frenne, De, Pieter, Florian Zellweger, Rodríguez-Sánchez, Francisco, Scheffers, Brett R., Hylander, Kristoffer, Luoto, Miska, Vellend, Mark, Verheyen, Kris, Lenoir, Jonathan, 2019. Global buffering of temperatures under forest canopies. Nature Ecol. Evolut. 3 (5), 744–749. https://doi.org/10.1038/s41559-019-0842-1.

Google, 2021. Introduction | Google Earth Engine API. Google Developers (blog). https://developers.google.com/earth-engine/.

Gorelick, Noel, Hancher, Matt, Dixon, Mike, Ilyushchenko, Simon, Thau, David, Moore, Rebecca, 2017. Google earth engine: planetary-scale geospatial analysis for everyone. Remote Sens. Environ. 202, 18–27. https://doi.org/10.1016/j.rse.2017.06.031.

Grossiord, Charlotte, Buckley, Thomas N., Cernusak, Lucas A., Novick, Kimberly A., Poulter, Benjamin, Siegwolf, Rolf T.W., Sperry, John S., McDowell, Nate G., 2020. Plant responses to rising vapor pressure deficit. New Phytol. 226 (6), 1550–1566. https://doi.org/10.1111/nph.16485.

Hamberg, L. Jonas, Fraser, Roydon A., Robinson, Derek T., Trant, Andrew J., Murphy, Stephen D., 2020. Surface temperature as an Indicator of plant species diversity and restoration in oak woodland. Ecol. Indic. 113, 106249.

Hatfield, Jerry L., Prueger, John H., 2015. Temperature extremes: effect on plant growth and development. Weather Climate Extremes 10, 4–10. https://doi.org/10.1016/j.wace.2015.08.001 (USDA Research and Programs on Extreme Events).

Hesslerová, Petra, Huryna, Hanna, Pokorný, Jan, Procházka, Jan, 2018. The effect of Forest disturbance on landscape temperature. Ecol. Eng. 120, 345–354.

Hesslerová, Petra, Pokorný, Jan, Huryna, Hanna, Harper, David, 2019. Wetlands and forests regulate climate via evapotranspiration. In: An, Shuqing, Verhoeven, Jos T.A. (Eds.), Wetlands: Ecosystem Services, Restoration and Wise Use, Ecological Studies. Springer International Publishing, Cham, pp. 63–93. https://doi.org/10.1007/978-3-030-14861-4_4.

Ibisch, P.L., Kriewald, S., Blumröder, J.S., 2019. Hambacher Forst in Der Krise Studie Zur Beurteilung Der Mikro- Und Mesoklimatischen Situation Sowie Randeffekten. Greenpeace e.V, Hamburg. https://www.greenpeace.de/sites/www.greenpeace.de/files/hambacher_forst_ii.pdf.

Ibisch, Pierre L., Kloiber, Judith, Hoffmann, Monika T. (Eds.), 2018. Barnim-Atlas. Lebensraum Im Wandel Eine Ökosystembasierte Betrachtung Des Barnims Zum Wohle Der Menschen. Ehm Welk, Schwedt.

Jarvis, A., Guevara, E., Reuter, H.I., Nelson, A.D., 2008. Hole-Filled SRTM for the Globe: Version 4. [Data Set]. http://srtm.csi.cgiar.org.

Jin, Menglin, Dickinson, Robert E., 2010. Land surface skin temperature climatology: benefitting from the strengths of satellite observations. Environ. Res. Lett. 5 (4), 044004 https://doi.org/10.1088/1748-9326/5/4/044004.

Kupika, Olga Laiza, Gandiwa, Edson, Nhamo, Godwell, Kativu, Shakkie, 2019. Local ecological knowledge on climate change and ecosystem-based adaptation strategies promote resilience in the middle Zambezi biosphere reserve, Zimbabwe. Scientifica 2019 (March), e3069254. https://doi.org/10.1155/2019/3069254.

Laurance, William F., Laurance, Susan G., Delamonica, Patricia, 1998. Tropical forest fragmentation and greenhouse gas emissions. For. Ecol. Manag. 110 (1), 173–180. https://doi.org/10.1016/S0378-1127(98)00291-6.

Li, Yan, Zhao, Maosheng, Motesharrei, Safa, Qiaozhen, Mu, Kalnay, Eugenia, Li, Shuangcheng, 2015. Local cooling and warming effects of forests based on satellite observations. Nat. Commun. 6 (1), 6603. https://doi.org/10.1038/ncomms7603.

Liu, Xiaohui, Zhang, Yuan, Dong, Guihua, Jiang, Ming, 2019. Difference in carbon budget from marshlands to transformed Paddy fields in the Sanjiang plain, Northeast China. Ecol. Eng. 137 (October), 60–64. https://doi.org/10.1016/j.ecoleng.2018.03.013.

Liu, Yanxu, Peng, Jian, Wang, Yanglin, 2018. Efficiency of landscape metrics characterizing urban land surface temperature. Landsc. Urban Plan. 180 (December), 36–53. https://doi.org/10.1016/j.landurbplan.2018.08.006.

Luber, George, McGeehin, Michael, 2008. Climate change and extreme heat events. Am. J. Prev. Med. 35 (5), 429–435. https://doi.org/10.1016/j.amepre.2008.08.021.

Lusiana, Betha, Kuyah, Shem, Öborn, Ingrid, van Noordwijk, Meine, 2017. Typology and metrics of ecosystem services and functions as the basis for payments, rewards and

co-investment. In: Coinvestment in Ecosystem Services: Global Lessons from Payment and Incentive Schemes. World Agroforestry Centre (ICRAF), Nairobi.
Maes, W.H., Pashuysen, Tom, Trabucco, Antonio, Veroustraete, Frank, Muys, Bart, 2011. Does energy dissipation increase with ecosystem succession? Testing the ecosystem exergy theory combining theoretical simulations and thermal remote sensing observations. Ecol. Model. 222 (23–24), 3917–3941.
Mildrexler, David J., Zhao, Maosheng, Running, Steven W., 2011. A global comparison between station air temperatures and MODIS land surface temperatures reveals the cooling role of forests. J. Geophys. Res. Biogeosci. 116 (G3) https://doi.org/10.1029/2010JG001486.
Mora, Camilo, Dousset, Bénédicte, Caldwell, Iain R., Powell, Farrah E., Geronimo, Rollan C., Bielecki, Coral R., Chelsie W. W. Counsell, et al., 2017. Global risk of deadly heat. Nat. Clim. Chang. 7 (7), 501–506. https://doi.org/10.1038/nclimate3322.
Nanfuka, Susan, Mfitumukiza, David, Egeru, Anthony, 2020. Characterisation of ecosystem-based adaptations to drought in the central cattle corridor of Uganda. African J. Range Forage Sci. 37 (4), 257–267. https://doi.org/10.2989/10220119.2020.1748713.
Norris, Catherine, Hobson, Peter, Ibisch, Pierre L., 2012. Microclimate and vegetation function as indicators of forest thermodynamic efficiency. J. Appl. Ecol. 49 (3), 562–570. https://doi.org/10.1111/j.1365-2664.2011.02084.x.
Novick, Kimberly A., Katul, Gabriel G., 2020. The duality of reforestation impacts on surface and air temperature. J. Geophys. Res. Biogeosci. 125 (4) https://doi.org/10.1029/2019JG005543.
Panagos, Panos, 2006. The European soil database. GEO: Connexion 5 (7), 32–33.
Parks, Peter J., Hardie, Ian W., 2018. Least-cost Forest carbon reserves: Cost-effective subsidies to convert marginal agricultural land to forests. In: Economics and Forestry, 1st ed. Routledge, p. 16. https://doi.org/10.4324/9781315182681-24.
Peng, Shu-Shi, Piao, Shilong, Zeng, Zhenzhong, Ciais, Philippe, Zhou, Liming, Li, Laurent Z.X., Myneni, Ranga B., Yin, Yi, Zeng, Hui, 2014. Afforestation in China cools local land surface temperature. Proc. Natl. Acad. Sci. 111 (8), 2915–2919. https://doi.org/10.1073/pnas.1315126111.
Pokorný, Jan, Hesslerová, Petra, Huryna, Hanna, Harper, David, 2016. Indirect and direct thermodynamic effects of wetland ecosystems on climate. In: Vymazal, Jan (Ed.), Natural and Constructed Wetlands: Nutrients, Heavy Metals and Energy Cycling, and Flow. Springer International Publishing, Cham, pp. 91–108. https://doi.org/10.1007/978-3-319-38927-1_7.
Pugh, Thomas A.M., Rademacher, Tim, Shafer, Sarah L., Steinkamp, Jörg, Barichivich, Jonathan, Beckage, Brian, Haverd, Vanessa, et al., 2020. Understanding the uncertainty in global Forest carbon turnover. Biogeosciences 17 (15), 3961–3989. https://doi.org/10.5194/bg-17-3961-2020.
R Core Team, 2021. R: The R Project for Statistical Computing. https://www.r-project.org/.
Ramsar Convention Secretariat, 2018. Global wetland outlook: State of the World's wetlands and their services to people. In: SSRN Scholarly Paper ID 3261606. Social Science Research Network, Rochester, NY. https://papers.ssrn.com/abstract=3261606.
Schneider, Eric D., Kay, James J., 1994. Complexity and thermodynamics: towards a new ecology. Futures 26 (6), 626–647. https://doi.org/10.1016/0016-3287(94)90034-5 (Special Issue Complexity: Fad or Future?).
Schumacher, Paul, Garstecki, Tobias, Mislimshoeva, Bunafsha, Morrison, John, Ibele, Benedikt, Lesk, Corey, Dzhumabaeva, Salamat, Bulbulshoev, Umed, Martin, Shaun, 2018. Using the open standards-based framework for planning and implementing ecosystem-based adaptation projects in the high mountainous regions of Central Asia. In: Alves, Fátima, Filho, Walter Leal, Azeiteiro, Ulisses (Eds.), Theory and Practice of Climate Adaptation, Climate Change Management. Springer International Publishing, Cham, pp. 23–48. https://doi.org/10.1007/978-3-319-72874-2_2.
Schwaab, Jonas, Davin, Edouard L., Bebi, Peter, Duguay-Tetzlaff, Anke, Waser, Lars T., Haeni, Matthias, Meier, Ronny, 2020. Increasing the broad-leaved tree fraction in European forests mitigates hot temperature extremes. Sci. Rep. 10 (1), 14153. https://doi.org/10.1038/s41598-020-71055-1.
Sheil, Douglas, 2018. Forests, atmospheric water and an uncertain future: the new biology of the global water cycle. Forest Ecosystems 5 (1), 1–22.
Shen, Xiangjin, Liu, Binhui, Jiang, Ming, Lu, Xianguo, 2020. Marshland loss warms local land surface temperature in China. Geophys. Res. Lett. 47 (6), e2020GL087648 https://doi.org/10.1029/2020GL087648.
Shen, Xiangjin, Jiang, Ming, Lu, Xianguo, Liu, Xingtu, Liu, Bo, Zhang, Jiaqi, Wang, Xianwei, et al., 2021. Aboveground biomass and its spatial distribution pattern of herbaceous marsh vegetation in China. Sci. China Earth Sci. 64 (7), 1115–1125. https://doi.org/10.1007/s11430-020-9778-7.
Su, Weizhong, Gu, Chaolin, Yang, Guishan, 2010. Assessing the impact of land use/land cover on urban heat island pattern in Nanjing City, China. J. Urban Plan. Dev. 136 (December), 365–372. https://doi.org/10.1061/(ASCE)UP.1943-5444.0000033.
Suggitt, Andrew J., Gillingham, Phillipa K., Hill, Jane K., Huntley, Brian, Kunin, William E., Roy, David B., Thomas, Chris D., 2011. Habitat microclimates drive fine-scale variation in extreme temperatures. Oikos 120 (1), 1–8. https://doi.org/10.1111/j.1600-0706.2010.18270.x.
Teuling, Adriaan J., Seneviratne, Sonia I., Stöckli, Reto, Reichstein, Markus, Moors, Eddy, Ciais, Philippe, Luyssaert, Sebastiaan, et al., 2010. Contrasting response of European forest and grassland energy exchange to heatwaves. Nat. Geosci. 3 (10), 722–727. https://doi.org/10.1038/ngeo950.
Teuling, Adriaan J., Van Loon, Anne F., Seneviratne, Sonia I., Lehner, Irene, Aubinet, Marc, Heinesch, Bernard, Bernhofer, Christian, Grünwald, Thomas, Prasse, Heiko, Spank, Uwe, 2013. Evapotranspiration amplifies European summer drought. Geophys. Res. Lett. 40 (10), 2071–2075. https://doi.org/10.1002/grl.50495.
Tran, Duy X., Pla, Filiberto, Latorre-Carmona, Pedro, Myint, Soe W., Caetano, Mario, Kieu, Hoan V., 2017. Characterizing the relationship between land use land cover change and land surface temperature. ISPRS J. Photogramm. Remote Sens. 124 (February), 119–132. https://doi.org/10.1016/j.isprsjprs.2017.01.001.
Van Liedekerke, Marc, Jones, Arwyn, Panagos, Panos, 2006. ESDBv2 Raster Library - a Set of Rasters Derived from the European Soil Database Distribution v2.0. European Commission; European Soil Bureau Network.
Vicedo-Cabrera, A.M., Scovronick, N., Sera, F., Royé, D., Schneider, R., Tobias, A., Astrom, C., et al., 2021. The burden of heat-related mortality attributable to recent human-induced climate change. Nat. Clim. Chang. 11 (6), 492–500. https://doi.org/10.1038/s41558-021-01058-x.
Wan, Z., Hook, S., Hulley, G., 2015. Collection-6MODIS land surface temperature ProductsUsers' guide. NASA EOSDIS Land Processes DAAC. https://doi.org/10.5067/MODIS/MYD11A1.006.
Weng, Qihao, Lu, Dengsheng, Schubring, Jacquelyn, 2004. Estimation of land surface temperature–vegetation abundance relationship for urban Heat Island studies. Remote Sens. Environ. 89 (4), 467–483. https://doi.org/10.1016/j.rse.2003.11.005.
Williams, A. Park, Allen, Craig D., Macalady, Alison K., Griffin, Daniel, Woodhouse, Connie A., Meko, David M., Thomas W. Swetnam, et al., 2013. Temperature as a potent driver of regional forest drought stress and tree mortality. Nat. Clim. Chang. 3 (3), 292–297. https://doi.org/10.1038/nclimate1693.
Wu, Yuxuan, Xi, Yi, Feng, Maoyuan, Peng, Shushi, 2021. Wetlands cool land surface temperature in tropical regions but warm in boreal regions. Remote Sens. 13 (8), 1439. https://doi.org/10.3390/rs13081439.
Wu, Zhijie, Zhang, Yixin, 2019. Water Bodies' cooling effects on urban land daytime surface temperature: ecosystem service reducing Heat Island effect. Sustainability 11 (3), 787. https://doi.org/10.3390/su11030787.
Xiao, Honglin, Weng, Qihao, 2007. The impact of land use and land cover changes on land surface temperature in a karst area of China. J. Environ. Manag. 85 (1), 245–257. https://doi.org/10.1016/j.jenvman.2006.07.016.
Yuan, Fei, Bauer, Marvin E., 2007. Comparison of impervious surface area and normalized difference vegetation index as indicators of surface urban Heat Island effects in Landsat imagery. Remote Sens. Environ. 106 (3), 375–386. https://doi.org/10.1016/j.rse.2006.09.003.
Zaitchik, Benjamin F., Macalady, Alison K., Bonneau, Laurent R., Smith, Ronald B., 2006. Europe's 2003 heat wave: a satellite view of impacts and land–atmosphere feedbacks. Int. J. Climatol. 26 (6), 743–769. https://doi.org/10.1002/joc.1280.
Zellweger, Florian, Coomes, David, Lenoir, Jonathan, Depauw, Leen, Maes, Sybryn L., Wulf, Monika, Keith J. Kirby, et al., 2019. Seasonal drivers of Understorey temperature buffering in temperate deciduous forests across Europe. Glob. Ecol. Biogeogr. 28 (12), 1774–1786. https://doi.org/10.1111/geb.12991.
Zeng, Zhenzhong, Piao, Shilong, Laurent Z. X. Li, Liming Zhou, Philippe Ciais, Tao Wang, Yue Li, et al., 2017. Climate mitigation from vegetation biophysical feedbacks during the past three decades. Nat. Clim. Chang. 7 (6), 432–436. https://doi.org/10.1038/nclimate3299.